TMT-based Quantitative Proteomic Analysis Reveals Defense Mechanism of Wheat Against the Crown Rot Pathogen Fusarium Pseudograminearum

Fangfang Qiao
Henan Agricultural University https://orcid.org/0000-0002-8742-9613
Xiwen Yang
Henan Agricultural University
Fengdan Xu
Henan Agricultural University
Yuan Huang
Henan Agricultural University
Jiemei Zhang
Henan Agricultural University
Miao Song
Henan Agricultural University
Sumei Zhou
Henan Agricultural University
Dexian He
Henan Agricultural University
Meng Zhang (zm2006@126.com)
College of Plant Protection, Henan Agricultural University, Zhengzhou, Henan 450002, China.

Research article

Keywords: Wheat (Triticum aestivum L.), Crown rot, Fusarium pseudograminearum, TMT, Differentially expressed proteins (DEPs), Defense mechanism

Posted Date: November 4th, 2020

DOI: https://doi.org/10.21203/rs.3.rs-100134/v1

Version of Record: A version of this preprint was published on February 8th, 2021. See the published version at https://doi.org/10.1186/s12870-021-02853-6.

Abstract

Background: Fusarium crown rot a major disease in wheat. However, wheat defense mechanisms remain poorly understood.

Results: In this study, we employed tandem mass tag (TMT) quantitative proteomics technology for one disease-susceptible (UC1110 (S1)) and one disease-tolerant wheat cultivar (PI610750 (S2)) inoculated with *Fusarium pseudograminearum* WZ-8A. Analysis of morphology and physiology showed that average seedling root diameter was significantly decreased 3 days post-inoculation (dpi) in both cultivars. Malondialdehyde content decreased in PI610750 and catalase activity increased in UC1110, indicating that morphology, physiology, and biochemistry differed in both cultivars in response to disease. TMT analysis identified 366 differentially expressed proteins (DEPs) by Gene Ontology enrichment and the Kyoto Encyclopedia of Genes and Genomes in the two comparison groups, S1-3dpi/S1-0dpi (163) and S2-3dpi/S2-0dpi (203). We concluded that phenylpropanoid biosynthesis (8), secondary metabolite biosynthesis (12), linolenic acid metabolites (5), glutathione metabolism (8), plant hormone signal transduction (3), MAPK signaling pathway-plant (4), and photosynthesis (12) contributed to wheat defense mechanisms. Protein-protein interaction network analysis showed that DEPs interacted in sugar metabolism and photosynthesis pathways. We validated 16 genes by real-time quantitative polymerase chain reaction.

Conclusion: The results were consistent with proteomics data. Our results provided insight into molecular mechanisms of interaction between wheat and *F. pseudograminearum*.

Background

Wheat (*Triticum aestivum* L.) is a major global food crop. Fusarium crown rot (FCR), caused by *Fusarium pseudograminearum*, is a major problem in wheat production. *F. pseudograminearum* is one of the most devastating plant pathogens among soil-borne diseases. *F. pseudograminearum* can absorb nutrients from major winter cereals to colonize [1]. The colonization of *F. pseudograminearum* initiates through epidermal penetration, most often through stomatal apertures, and progresses into the parenchymatous hypoderm. Hyphae spread from the culm base vertically through the tissues, initially through the hypoderm and pith cavity in culm tissues [2]. This pathogen mainly affects wheat, durum (*Triticum turgidum* L. spp. durum (Dest.)), and barley (*Hordeum vulgare* L.) [3]. Although oats (*Avena sativa* L.) can be infected, they show few or no symptoms of disease [4]. In the Pacific Northwest and Australia, yield loss can be up to 10–35% under natural inoculum levels [5–7]. According to reports, *F. pseudograminearum* also causes wheat crown rot in China, and the environmental conditions are especially suitable for *F. pseudograminearum* in Henan, the largest wheat production province. This pathogen may cause serious harm to wheat production in the future [8]. Fully disease-resistant or immune cultivars have not been found in common wheat. Therefore, improving the genetic resistance of wheat to crown rot is an important objective.

Previously studies constructed a genetic map of *F. pseudograminearum* and completed a genomic sequence [9, 10]. Zhou et al. investigated the distribution and diversity of the pathogens associated with Fusarium crown rot in the Huanghuai wheat-growing region of China and found that *F. pseudograminearum* was the dominant species [11]. Several studies have confirmed that ER Lumenal Hsp70 protein FpLhs1, transcription factor FpAda1, and FpNPS9 are important for *F. pseudograminearum* infection [12–14]. FCR resistance responses in wheat are complex and controlled by multiple quantitative trait loci (QTLs) [15]. Thus, some studies have focused on the identification of gene loci in wheat and barley that are resistant to crown rot [16, 17]. Among them, Yang et al. used a bi-parental population derived from the wheat cultivars UC1110 and PI610750 and detected three QTLs on chromosome 6A [18]. In addition, it has been reported that *F. pseudograminearum* produces a new class of active cytokinin that could activate plant cytokinin signaling during infection [19]. These molecules may extensively reprogram the host environment through crosstalk with defense hormone signaling pathways [20, 21].

With regard to plant defense responses triggered by *F. pseudograminearum*, host–pathogen interactions have been studied by transcriptome analyses in wheat using an Affymetrix gene chip [22]. It has been suggested that differentially expressed genes were involved in antibacterial defense, oxidative stress, and signal transduction, as well as in primary and secondary metabolism [22]. Some defense-related genes were induced faster in the FCR-resistant cultivar Sunco than in the susceptible cultivar Kennedy [23]. In addition, many of the *F. pseudograminearum*-responsive genes are altered by toxin deoxynivalenol and plant defense–related hormones, which prevent *F. pseudograminearum* infection in wheat plants [22]. A combination of transcriptomics and metabolomics also has been used to study defense responses, and genes related to pathogen recognition and signal transduction, transcription factors, cell transport, and detoxification have been discovered [24].

Currently, little is known about the dynamics of proteomics and metabolomics in infected host plants. Proteomics research focused on resistance to *F. pseudograminearum* in wheat is not yet available. In this study, we selected wheat cultivars with tolerance and susceptibility to *F. pseudograminearum* as the research materials. We analyzed protein expression abundance in the wheat after *F. pseudograminearum* infection using tandem mass tag (TMT) quantitative proteomics technology. Our objectives were to clarify how these proteins participate in resistance and to gather information on inducible defense mechanisms in response to *F. pseudograminearum*. We also expected that this study would provide a new perspective for germplasm innovation regarding resistance to *F. pseudograminearum* in wheat, as well as for genetic improvement and the breeding of new cultivars.

Results

Impact of *F. pseudograminearum* stress on wheat growth and development

The results showed that *F. pseudograminearum* stress significantly affected the growth and development of wheat seedlings, especially the root system (Figure 1a–1h). At 3 days post-inoculation (dpi), the light brown symptoms of disease initially appeared at the stem bases of susceptible cultivar UC1110, which indicated that the incubation period was over. (Figure 1a, 1b). According to our observations, the average root diameters of UC1110 and PI610750 seedlings were both significantly decreased by 12.5% and 18.5% at 3 dpi compared with 0 dpi, respectively (Figure 1f), whereas total root length, total root surface area, total root volume, and forks were significantly increased (Figure 1c–1e, 1g, 1h). The average number of root tips of UC1110 and PI610750 seedlings were both significantly increased by 70.2% and 123.5% at 3 dpi compared with 0 dpi, respectively.

The results of these physiological experiments showed that compared with those of 0 dpi seedlings, the root vigor, leaf total chlorophyll content, root soluble protein content, and root superoxide dismutase (SOD) activity of 3 dpi UC1110 wheat seedlings were significantly increased by 43.9%, 27.0%, 74.1%, and 91.9%, respectively, as well as in PI610750, where these values were increased by 102.4%, 33.3%, 123.2%, and 42.4%, respectively (Figure 2a, 2c–2e). The extent of these increases was higher in PI610750 than in UC1110. The activity of root peroxidase (POD) in UC1110 and PI610750 wheat seedlings, however, was significantly decreased at 3 dpi (Figure 2f). In addition, the root soluble sugars and malondialdehyde (MDA) content of PI610750 wheat seedlings were significantly decreased by 17.3% and 18.0% at 3 dpi, respectively (Figure 2b, 2h), whereas the root catalase (CAT) activity of UC1110 wheat seedlings was significantly increased by 79.8% (Figure 2g). Together, these results indicated that there were certain differences in the morphological, physiological, and biochemical responses of disease-tolerant cultivar PI610750 and disease-susceptible cultivar UC1110 under *F. pseudograminearum* stress.

Identification of DEPs in response to *F. pseudograminearum* infection

We comprehensively examined and identified defense-related proteins of stem bases of two wheat cultivars, UC1110 and PI610750, under *F. pseudograminearum* stress using TMT quantitative proteomics technology. We selected the stem bases of wheat for proteomic analysis in this experiment because they represent the first obstacle to the invasion of the crown rot pathogen *F. pseudograminearum*.

To investigate the mechanisms of the differences in resistance of UC1110 and PI610750 at the protein level after *F. pseudograminearum* inoculation, we compared two groups, that is, S1-3dpi/S1-0dpi and S2-3dpi/S2-0dpi, using TMT quantitative proteomics study. Compared with the S1-0dpi treatment, we identified 163 differentially expressed proteins (DEPs) in the S1-3dpi treatment, including 75 up-regulated and 88 down-regulated protein species, of which 100 protein species were specifically expressed in this group (Figure 3 and Figure 4). In S2-3dpi/S2-0dpi, 203 protein species were differentially expressed, containing 133 up-regulated and 70 down-regulated proteins, of which 140 proteins were specifically expressed in this group. A total of 63 proteins were common in S1-3dpi/S1-0dpi and S2-3dpi/S2-0dpi, including 23 up-regulated and 40 down-regulated proteins in S1-3dpi/S1-0dpi and 22 up-regulated and 41 down-regulated proteins in S2-3dpi/S2-0dpi (Figure 4).

Cluster analysis of DEPs based on GO enrichment

To determine their potential functions, we annotated 366 DEPs by Gene Ontology (GO). GO functional enrichment analysis showed that 186, 126, and 161 protein species were enriched in biological processes, cellular components, and molecular function, respectively (Supplementary Table S1).

Enrichment of DEPs related to biological processes

Under biological processes, the common DEPs (C1) in the two comparison groups of S1-3dpi/S1-0dpi and S2-3dpi/S2-0dpi were significantly enriched in the terms of organic acid catabolism, cell wall polysaccharide metabolism, and cell wall macromolecule metabolism (Figure 5a). The specific DEPs (C2) of S1-3dpi/S1-0dpi were significantly enriched in the terms of negative regulation of hydrolase activity, dephosphorylation, regulation of proteolysis, negative regulation of protein metabolism, negative regulation of cellular metabolism, organic acid biosynthesis, carboxylic acid metabolism, oxoacid metabolism, and negative regulation of macromolecule metabolism (Figure 5a). The specific DEPs (C3) of S2-3dpi/S2-0dpi were significantly enriched in the terms of cellular protein metabolism, photosynthesis (dark reaction), carbohydrate biosynthesis, cellular macromolecule biosynthesis, the photosynthetic electron transport chain, polysaccharide biosynthesis, lipid transport, cellular carbohydrate biosynthesis, hexose metabolism, cellular polysaccharide metabolism, photosynthesis (light harvesting), amide biosynthesis, peptide biosynthesis, and peptide metabolism (Figure 5a). This analysis showed that the DEPs related to organic acid catabolism and cell wall metabolism responded to *F. pseudograminearum* stress in the seedling stem bases of both susceptible and tolerant cultivars. The disease-susceptible cultivar UC1110 also responded to stress through the DEPs related to dephosphorylation and carboxylic acid metabolism, and the disease-tolerant cultivar PI610750 mainly through the DEPs related to photosynthesis and sugar metabolism.

Enrichment of DEPs related to cellular components

In the cellular components category, the common DEPs (C1) in the two comparison groups of S1-3dpi/S1-0dpi and S2-3dpi/S2-0dpi were significantly enriched in the terms of cell walls, external encapsulating structures, the cell periphery, and extracellular regions (Figure 5b). The specific DEPs (C2) of S1-3dpi/S1-0dpi were significantly enriched in apoplasts (Figure 5b). The specific DEPs (C3) of S2-3dpi/S2-0dpi were significantly enriched in the terms of plastid thylakoids, chloroplast thylakoids, the photosystem, photosynthetic membranes, cytoplasmic parts, thylakoid membranes, ribosomes, the ribonucleoprotein complex, cytoplasm, the membrane protein complex, and organelles (Figure 5b). This analysis showed that the DEPs related to the cell wall first responded to *F. pseudograminearum* stress in the seedling stem bases of both susceptible and tolerant cultivars. The disease-susceptible cultivar UC1110 also responded to stress through the DEPs related to apoplasts, and the disease-tolerant cultivar PI610750 mainly through the DEPs related to chloroplasts.

Enrichment of DEPs related to molecular function

In terms of molecular function, the common DEPs (C1) in the two comparison groups of S1-3dpi/S1-0dpi and S2-3dpi/S2-0dpi were significantly enriched in the terms of glucosidase activity, hydrolase activity, phosphatidylcholine1-acylhydrolase activity, cysteine-type peptidase activity, phospholipase activity, lipase activity, and carboxylic ester hydrolase activity (Figure 5c). The specific DEPs (C2) of S1-3dpi/S1-0dpi were significantly enriched in the terms of peptidase regulator activity, endopeptidase regulator activity, phosphatase activity, oxidoreductase activity, nitronate monooxygenase activity, flavin mononucleotide binding, hydrolase activity, enzyme inhibitor activity, transferase activity, dioxygenase activity, and acid phosphatase activity (Figure 5c). The specific DEPs (C3) of S2-3dpi/S2-0dpi were significantly enriched in the terms of electron transporter activity, electron carrier activity, ribulose-bisphosphate carboxylase activity, cellulose synthase activity, glucosyltransferase activity, metal cluster binding, protein heterodimerization activity, oxidoreductase activity, lipid binding, tetrapyrrole binding, structural constituents of ribosomes, structural molecule activity, and chlorophyll binding (Figure 5c). This analysis showed that the disease-tolerant cultivar PI610750 mainly responded to stress through the DEPs related to electron transporter activity, electron carrier activity, cellulose synthase activity, and oxidoreductase activity in the process of plant-pathogen interaction.

Kyoto Encyclopedia of Genes and Genomes pathway enrichment analysis of DEPs

Further analysis using Kyoto Encyclopedia of Genes and Genomes (KEGG) pathway enrichment showed that all DEPs of the two comparison groups were significantly enriched in in the terms of ribosomes (20%), phenylpropanoid biosynthesis (14%), photosynthesis (11%), glutathione metabolism (11%), carbon fixation in photosynthetic organisms (7%), alpha-linolenic acid metabolism (7%), glyoxylate and dicarboxylate metabolism (7%), linoleic acid metabolism (6%), cyanoamino acid metabolism (6%), photosynthesis-antenna proteins (6%), and flavone and flavonol biosynthesis (5%) (Supplementary Figure S1). The 63 common DEPs (C1) in the two comparison groups of S1-3dpi/S1-0dpi and S2-3dpi/S2-0dpi were significantly enriched in the terms of biosynthesis of secondary

metabolites (osa01110), phenylpropanoid biosynthesis (osa00940), protein processing in endoplasmic reticulum (osa04141), starch and sucrose metabolism (osa00500), and cyanoamino acid metabolism (osa00460) (Figure 6, Supplementary Table S2).

The specific DEPs (C2) of S1-3dpi/S1-0dpi were significantly enriched in the terms of linoleic acid metabolism (osa00591), glutathione metabolism (osa00480), alpha-linolenic acid metabolism (osa00592), MAPK signaling pathway-plant (osa04016), flavone and flavonol biosynthesis (osa00944), and ubiquinone and other terpenoid-quinone biosynthesis (osa00130) (Figure 6, Supplementary Table S3). The specific DEPs (C3) of S2-3dpi/S2-0dpi were significantly enriched in the terms of ribosomes (osa03010), photosynthesis (osa00195), photosynthesis-antenna proteins (osa00196), flavone and flavonol biosynthesis (osa00944), carbon fixation in photosynthetic organisms (osa00710), and glyoxylate and dicarboxylate metabolism (osa00630) (Figure 6, Supplementary Table S4). This analysis showed that the DEPs related to secondary metabolites, protein processing, and energy metabolism pathways responded to stress in the seedling stem bases of both susceptible and tolerant cultivars. The susceptible cultivar UC1110 responded to stress mainly through the DEPs related to linoleic acid metabolism and glutathione metabolism, and the disease-tolerant cultivar PI610750 mainly through the DEPs related to photosynthesis and glyoxylic acid and dicarboxylate metabolism.

Interaction network analysis of *F. pseudograminearum*-responsive proteins in wheat

The present study used the online STRING database and Cytoscape software to construct a protein-protein interaction network for all DEPs of the two comparison groups in response to *F. pseudograminearum*. This network showed that 76 of the possible DEPs interacted. With the MCODE plug-in toolkit, three enriched interaction clusters were associated with ribosomes, photosynthesis, and sugar metabolism (Figure 7). Sixteen interaction proteins belonged to the ribosome network. These proteins included 15 up-regulated proteins and one down-regulated protein in the comparison group S2-3dpi/S2-0dpi. Seven interaction proteins belonged to the carbohydrate metabolic process network, including four down-regulated proteins in the two comparison groups of S1-3dpi/S1-0dpi and S2-3dpi/S2-0dpi, and one down-regulated and two up-regulated proteins in the comparison group of S2-3dpi/S2-0dpi. Three interaction proteins belonged to the photosynthesis network, including three up-regulated proteins in S2-3dpi/S2-0dpi. Other information about proteins is shown in Table S5.

Correlation between mRNA and protein abundance

To further validate the reliability of the proteomics data, we selected 16 genes for quantitative real time–polymerase chain reaction (qRT-PCR) analysis. Three common genes in the two comparison groups showed similar tendencies as those for protein expression, including NMT1, GLU1B, and XIPI. In the comparison group of S1_3dpi/sS1_0dpi, NMT1 and GLU1B were up-regulated and down-regulated, respectively. In the comparison group of S2_3dpi/S2_0dpi, however, both XIPI and GLU1B were down-regulated (Table 1). In the comparison group of S1_3dpi/S1_0dpi, five specific DEPs were up-regulated at both the transcription and translation levels. Similarly, in the comparison group of S2_3dpi/S2_0dpi, eight specific DEPs were up-regulated at both the transcription level and translation level. The primer sequences for 16 genes are listed in Supplementary Table S6.

Discussion

The two wheat cultivars with different levels of disease tolerance showed obvious differences in morphology, physiology, and biochemistry in response to the crown rot pathogen *F. pseudograminearum*. The average root diameter in both cultivars decreased. The root soluble sugars and root MDA content decreased in PI610750, and the CAT activity increased in UC1110. Meanwhile, increases in root vigor, root soluble protein content, and root SOD activity were higher at 3 dpi in PI610750 than in UC1110. This showed that the defense mechanism of wheat to the crown rot pathogen *F. pseudograminearum* was complicated. Although many factors related to crown rot resistance have been identified, the detailed molecular mechanisms of crown rot resistance are still poorly understood [1]. Therefore, understanding the defense mechanism of wheat against crown rot is crucial to the sustainable improvement of wheat yield and quality. The DEPs of the two cultivars studied were associated with metabolic pathways, plant-pathogen interaction, and photosynthesis.

Metabolic pathways in response to *F. pseudograminearum* infection

The metabolic pathway of wheat in response to *F. pseudograminearum* is essential, accounting for 37% of DEPs in all KEGG pathways. Previous studies have shown that proline metabolism is implicated in plant response to abiotic stress, and proline dehydrogenase (ProDH) is the first step to catalyze the degradation of proline [25]. According to reports, 4-hydroxy-7-methoxy-3-oxo -3,4-dihydro-2H-1,4-benzoxazine-2-yl glucoside β-D-glucosidase is a typical member of the metabolic pathway, because 4-hydroxy-7-methoxy-3-oxo-3,4-dihydro-2H-1,4-benzoxazin-2-yl glucoside β-D-glucosidase is involved in the metabolism of high-energy compounds and plant growth [26]. Regarding β-glucosidase, some studies have shown that it is involved in catalyzing the hydrolysis of glycosides and releasing glucose into the glycolysis process [27]. In plants, glutathione S-transferases (GSTs) have been shown to play a major role in cell detoxification and stress tolerance [28–30]. Previously, it was reported that lipoxygenase, allene oxide cyclase, and allene oxide synthase (AOS) are three important enzymes in jasmonic acid (JA) biosynthesis, and that the activation of AOS enhances the drought tolerance of chickpea [31–33]. Studies also have shown that AOS transcripts and JA concentration in cells are critical for responses to pathogen and virus infection in plants [34, 35].

Some studies have indicated that NADH-dependent glutamate synthetase (NADH-GOGAT) is located in non-green tissues and highly expressed in roots, participates in the ammonium assimilation pathway, and promotes the absorption of nitrogen by plants [36]. Previous research has shown that the two enzymes phenylalanine ammonia lyase and cinnamoyl-CoA reductase are mainly involved in lignin biosynthesis. The biosynthesis of lignin is a major branch of phenylpropane biosynthesis, and the biosynthesis of phenylpropane is involved in the resistance of plants to diseases [37–39]. In this study, we found five common DEPs in the two comparison groups of S1-3dpi/S1-0dpi and S2-3dpi/S2-0dpi to be significantly down-regulated, including ProDH, 4-hydroxy-7-methoxy-3-oxo-3,4-dihydro-2H-1,4-benzoxazin-2-yl glucoside beta-D-glucosidase, Beta-glucosidase 26, AOS, and GSTU1. ProDH, AOS, and GSTU1 were enriched in the KEGG pathways of arginine and proline metabolism (osa00330), alpha-Linolenic acid metabolism (osa00592), and glutathione metabolism (osa00480), respectively.

In addition, 4-hydroxy-7-methoxy-3-oxo-3,4-dihydro-2H-1,4-benzoxazin-2-yl glucoside beta-D-glucosidase and beta-glucosidase 26 were enriched in the three pathways of starch and sucrose metabolism (osa00500), cyanoamino acid metabolism (osa00460), and phenylpropanoid biosynthesis (osa00940) in the two comparison groups S1-3dpi/S1-0dpi and S2-3dpi/S2-0dpi. GSTU6 and NADH-GOGAT were up-regulated and were enriched in the pathways of glutathione metabolism (osa00480) and nitrogen metabolism (osa00910), respectively. Cinnamoyl-CoA reductase 1, peroxidase, and phenylalanine ammonia-lyase also were up-regulated and were enriched in the pathway of phenylpropanoid biosynthesis (osa00940). This showed the following: (1) ProDH and 4-hydroxy-7-methoxy-3-oxo-3,4-dihydro-2H-1,4-benzoxazine-2-yl glucoside βD-glucoside enzymes play an important role in the defense mechanism of wheat against *F. pseudograminearum*; (2) the study of GSTs in two wheat cultivars may reveal the differences in the role of GSTU1 and GSTU6 in the defense mechanism of wheat against *F. pseudograminearum*; (3) the down-regulation of AOS in the JA pathway makes UC1110 more susceptible to pathogen infection; (4) cinnamoyl-CoA reductase 1, peroxidase, and phenylalanine ammonia lyase were up-regulated in the biosynthesis of phenylpropane, which is highly related to plant defense ability; and (5) the metabolic pathways of plants in response to pathogenic stress are complex and changeable (Figure 8).

Plant-pathogen interactions in wheat

Plants have various defense mechanisms. These include the production of antimicrobial peptides, particularly pathogenesis-related proteins (PR proteins). PR proteins were first noted in plants as part of the hypersensitive response but have since been assigned an array of biological roles [40]. PR proteins are a type of stress-responsive protein whose expression can be induced by pathogen invasion [41]. A number of studies have shown that PR proteins participate in plant defense mechanisms as many of them are endowed with antimicrobial activity against plant pathogens, with different antifungal, antibacterial, and antiviral effects [42, 43]. Regarding the specific DEPs in the comparison group of S1_3dpi/S1_0dpi, multiple PR proteins related to plant-pathogen interactions were identified, including PR protein-1.2, PR protein 1-1, and PR protein 1-2. The expression levels of these proteins were up-regulated in response to *F. pseudograminearum* infection.

PR protein 1 is an antimicrobial protein in host defense that is targeted by plant pathogens during infection [44–46][44-46]. Production of the PR proteins in response to pathogen invasion is related to the plant disease resistance specialized in system-acquired resistance (SAR) [47]. PR-1-5 is a potential target of ToxA, and the site-specific interaction between PR-1-5 and ToxA may mediate ToxA-induced necrosis of susceptible wheat [48]. In this study, pathogenesis-related (PR-1.2, Pr-1-1, Pr-1-2) proteins were up-regulated in the comparison group of S1_3dpi/sS1_0dpi and involved in plant hormone signal transduction (osa04075) and the MAPK signal plant pathway (osa04016), suggesting that the PR1 family plays an important role in the crown rot defense mechanism of wheat.

Defensive photosynthetical activities of wheat stem bases infected by *F. pseudograminearum*

In plants, chloroplast photosynthesis is an important biochemical reaction that converts light energy into chemical energy to maintain plant life [49]. Regarding plant defense and photosynthesis, research has indicated that the rate of photosynthesis is reduced after pathogen invasion, such as in barley with powdery mildew, potato with *Phytophthora infestans*, and soybean with *Phytophthora sojae* [50–52]. In this study, the specific DEPs in the comparison group of S2_3dpi/S2_0dpi were significantly enriched in the three photosynthesis-related pathways of photosynthesis (osa00195), photosynthesis-antennary protein (osa00196), and carbon fixation (osa00710) (Figure 6). The increase in the abundance of photosynthesis-related proteins may reflect the fact that photosynthesis provides a large amount of energy for plant defense. Thus, photosynthesis-related proteins in the disease-tolerant cultivar PI610750 play an important role in disease defense.

Previous studies have shown that Sedoheptulose-1,7-bisphosphatase, phosphoribulokinase, glyceraldehyde-3-phosphate dehydrogenase, and ribulose 1,5-bisphosphate carboxylase/oxygenase (Rubisco) are involved in the Calvin cycle, and phosphoglycerate kinase participates in the glycolytic, gluconeogenic, and photosynthetic pathways [53, 54]. It also has been reported that increasing the activity of Sedoheptulose-1,7-bisphosphatase in transgenic tobacco plants can promote photosynthesis and growth from the early stages of development [55]. Rubisco is an enzyme complex in plants that is composed of eight large subunits and eight small subunits [56]. It has been reported that the abundance of the small and large subunits of Rubisco increased significantly in Zhongmu-1 8 h after salt treatment [57]. The increase in the abundance of Rubisco large subunits and the decrease in small subunits also been have found in nontransgenic wheat in response to drought [58, 59]. It has been reported that Rubisco large subunits and ribose-1 are down-regulated 24 h post-inoculation, and then are up-regulated 48 and 72 h post-inoculation [60].

In our study, we enriched Sedoheptulose-1,7-bisphosphatase, phosphoribulokinase, phosphoglycerate kinase, glyceraldehyde-3-phosphate dehydrogenase, Rubisco large subunits, and Rubisco small subunits in the carbon fixation pathway of photosynthetic organisms (osa00710) of PI610750. The increase in abundance of these DEPs indicated that photosynthesis plays a major role in the defense mechanisms of disease-tolerant cultivar PI610750. In summary, the disease-tolerant cultivar PI610750 may defend itself against diseases by increasing its photosynthetic rate, providing energy for plants.

Conclusions

Through TMT-based quantitative proteomic analysis, we confirmed that the physiological and biochemical responses of wheat disease-tolerant cultivar PI610750 and disease-susceptible cultivar UC1110 were significantly different under *F. pseudograminearum* stress. Based on the cluster analysis results of GO enrichment and KEGG pathway enrichment, the results indicated that the metabolic pathways of wheat in response to *F. pseudograminearum* stress are complex. The disease-tolerant cultivar PI610750 and the susceptible cultivar UC1110 interacted with pathogens during the incubation period. Although these cultivars shared many of the same metabolic pathways, they also had unique pathways. These unique pathways in the susceptible cultivar UC1110 were mainly related to linoleic acid metabolism, plant hormone signal transduction, MAPK signaling pathway – plant, and ubiquinone biosynthesis, while the unique pathways in the disease-tolerant cultivar PI610750 were mainly related to photosynthesis, carbon fixation in photosynthetic organisms, flavone and flavonol biosynthesis, and glyoxylate and dicarboxylate metabolism. The DEPs in seedling stem bases of the disease-susceptible cultivar UC1110 were mainly related to glutathione metabolism, nitrogen metabolism, and phenylpropane biosynthesis, whereas the DEPs in seedling stem bases of the disease-tolerant cultivar PI610750 were mainly related to photosynthesis. This fully demonstrated that there are differences in the defense mechanism of the disease-tolerant wheat cultivar PI610750 and the disease-susceptible cultivar UC1110 against *F. pseudograminearum*, which provides a perspective for wheat genetic improvement and breeding.

Methods

Experimental materials and inoculation

In these experiments, we used wheat cultivars UC1110 and PI 610750, provided by Prof. Jorge Dubcovsky from the University of California, Davis. The cultivar UC1110 is susceptible to the predominant Chinese isolate WZ-8A of *F. pseudograminearum*, whereas the cultivar PI 610750 is tolerant. UC1110 and PI 610750 seeds were sterilized by immersion in 75% (w/v) alcohol for 30 s and then thoroughly washed with distilled water. We grew sterilized seeds in the sterilized pot (12 cm × 17 cm) with 2 kg sterilized soil (sand: soil =

2.5:1). Seedlings were maintained in a growth chamber at 25/20°C day/night temperatures under a 16/8 h light/dark photoperiod and 65/75% day/night relative humidity.

We infected one-week old seedlings by *F. pseudograminearum* about 20 g millet matrix and used plants at 0 dpi as controls. We collected the stem bases of the two wheat cultivars at 0, 1, 2, and 3 dpi, until symptoms were visible, and then stored samples at -80°C until protein extraction. We performed three biological replicates per treatment (Figure 9).

Measurements of plant morphological and physiological parameters

We examined morphology using a V700Photo-root scanner and analyzed morphology parameters using the Win-RHIZO (LA6400XL, Regent Instruments Inc., Quebec, Canada) system, including total root length, total root surface area, total root volume, average root diameter, number of root tips, and number of forks. We collected wheat roots and leaves at different times (0, 1, 2, and 3 dpi). Root activity was determined by the TTC modified method, as described by Wang et al. and Cao et al. [61, 62]. We determined the content of total soluble sugar using a sulfuric acid-anthrone method [63, 64] and measured leaf chlorophyll content by spectrophotometry [65]. We measured the activity of enzymes related to stress, POD, SOD, and CAT according to previously described methods [65, 66] and measured the protein content using the Bradford method with bovine serum albumin (BSA) as the standard [67]. We determined malondialdehyde (MDA) content according to previously described methods [65].

Protein extraction

The sample was ground by liquid nitrogen into cell powder and then transferred to a 5 ml centrifuge tube. After that, we added four volumes of lysis buffer (8 M urea, 1% Triton-100, 10 mM dithiothreitol, and 1% Protease Inhibitor Cocktail) to the cell powder, followed by sonication three times on ice using a high-intensity ultrasonic processor (Scientz, Zhejiang, China). We removed the remaining debris by centrifugation at 20,000 g at 4°C for 10 min. Finally, the protein was precipitated with cold 20% TCA for 2 h at -20°C. After centrifugation at 12,000 g at 4°C for 10 min, the supernatant was discarded. We washed the remaining precipitate with cold acetone three times. The protein was re-dissolved in 8 M urea and the protein concentration was determined with a BCA kit according to the manufacturer's instructions.

Trypsin digestion

For digestion, we reduced the protein solution with 5 mM dithiothreitol for 30 min at 56°C and alkylated with 11 mM iodoacetamide for 15 min at room temperature in darkness. The protein sample was then diluted by adding 100 mM TEAB until the urea concentration was less than 2 M. Finally, we added trypsin at 1:50 trypsin-to-protein mass ratio for the first digestion overnight and 1:100 trypsin-to-protein mass ratio for a second 4 h digestion.

LC-MS (MS/MS) analysis

The tryptic peptides were dissolved in 0.1% formic acid (solvent A), directly loaded onto a homemade reversed-phase analytical column (15 cm length, 75 μm i.d.). The gradient increased from 6% to 23% solvent B (0.1% formic acid in 98% acetonitrile) over 26 min, increased from 23% to 35% in 8 min and climbed to 80% in 3 min, and then held at 80% for the last 3 min, all at a constant flow rate of 400 nL/min on an EASY-nLC 1000 ultra-performance liquid chromatography (UPLC) system. The peptides were subjected to NSI source followed by tandem mass spectrometry (MS/MS) in QExactiveTM Plus (ThermoFisher, Waltham, MA, USA) coupled online to the UPLC. The electrospray voltage applied was 2.0 kV. The m/z scan range was 350 to 1800 for a full scan, and intact peptides were detected in the Orbitrap at a resolution of 70,000. We then selected peptides for MS/MS using NCE set at 28. The fragments were then detected in the Orbitrap at a resolution of 17,500. We conducted a data-dependent procedure that alternated between one MS scan followed by 20 MS/MS scans with 15.0 s dynamic exclusion. We set the automatic gain control at 5E4. The fixed first mass was set at 100 m/z.

Database search

We processed the resulting MS/MS data using the Maxquant search engine (v.1.5.2.8). Tandem mass spectra were searched against the UniProt *Triticum aestivum* database concatenated with a reverse decoy database. Trypsin/P was specified as a cleavage enzyme

allowing up to two missing cleavages. The mass tolerance for precursor ions was set at 20 ppm in First search and 5 ppm in Main search, and the mass tolerance for fragment ions was set at 0.02 Da. Carbamidomethyl on Cys was specified as a fixed modification and oxidation on Met was specified as a variable modification. We adjusted the false discovery rate (FDR) to <1% and set the minimum score for peptides at >40. We selected TMT 6-plex for the protein quantification method. A global FDR was set at 0.01, and protein groups required at least two peptides to be considered for quantification. For protein quantification, we calculated the protein ratios as the median of only the unique peptides of the protein. All peptide ratios were normalized by the median protein ratio. We used cutoff values of more than 1.50-fold and less than 0.667-fold to identify up-regulated and down-regulated proteins at $p < 0.05$.

Bioinformatics analysis

We derived GO annotation proteome from the UniProt-GOA database (http://www.ebi.ac.uk/GOA/). We used the KEGG database to annotate protein pathways. We analyzed the protein–protein interactions for the identified proteins using the STRING v10.5 database (http://string-db.org) to determine their functions and pathways. We visualized interaction network form STRING in Cytoscape. We used a graph theoretical clustering algorithm, molecular complex detection (MCODE) to analyze densely connected regions. MCODE is part of the plug-in toolkit of the network analysis and visualization software Cytoscape.

Quantitative real-time reverse transcription–polymearase chain reaction

We extracted the total RNA of wheat stem bases using the TaKaRa MiniBEST Plant RNA Extraction Kit (TaKaRa, Dalian, China). To digest the genomic DNA, we added RNase-free DNaseI to each sample. We performed reverse transcription was performed following the kit instructions (Promega Corp., Madison, WI, USA). cDNAs were stored at -20°C for real-time PCR amplification. The gene primers were designed by Primer 5.0 and are shown in Supplemental Table S1. We conducted qRT-PCR in 20 ml volumes containing 2 ml 50-fold diluted cDNA, 0.4 ml of each primer (forward and reverse), 7.2 ml of nuclease-free water, and 10 ml of GoTaq® qPCR Master Mix (Perfect Real Time; Promega). PCR conditions were 95°C for 3 min, 45 cycles of 10 s at 95°C, 60°C for 30 s, and 72°C for 20 s. Three biological replicates of each sample were performed to guarantee the reproducibility of the results. We performed the reactions in a CFX96 Real-Time PCR Detection System (Bio-Rad Laboratories, Inc., Hercules, CA, USA). We analyzed all data using CFX Manager Software (Bio-Rad Laboratories, Inc.). The relative expression levels were calculated using the $2^{-\Delta\Delta CT}$ method [68]. β-actin was used as an internal control gene.

Statistical analyses

We performed statistical analyses for morphological results across ten biological replicates, for physiological and biochemical analyses across four biological replicates, and for proteomic analyses across three biological replicates. We performed analysis of variance using IBM SPSS Statistics 23.0 (IBM Corp., Armonk, NY, USA). Data are presented as means ± standard deviation (SD) values. We determined the statistical significance of Student's t-tests at a $P < 0.05$ threshold.

List Of Abbreviations

TMT: Tandem mass tag; S1: UC1110; S2: PI610750; dpi: Days post inoculation; DEPs: Differentially expressed proteins; FCR: Fusarium crown rot; QTLs: Quantitative trait loci; SOD: Superoxide dismutase; POD: Peroxidase; MDA: Malondialdehyde; CAT: Catalase; GO: Gene Ontology; KEGG: Kyoto Encyclopedia of Genes and Genomes; qRT-PCR: Quantitative real time–polymerase chain reaction; ProDH: Proline dehydrogenase; GSTs: Glutathione S-transferases; AOS: Allene oxide synthase; JA: Jasmonic acid; NADH-GOGAT: NADH-dependent glutamate synthetase; PR proteins: Pathogenesis-related proteins; SAR: System-acquired resistance; FDR: False discovery rate

Declarations

Ethics approval and consent to participate

Not applicable.

Consent for publication

Not applicable.

Availability of data and materials

Not applicable. The datasets used and/or analyzed during the current study are available from the corresponding author on request.

Competing interests

The authors declare that they have no competing interest.

Funding

The work was supported National Key Research and Development Program "Science and Technology Innovation of High Grain Production Efficiency" of China (2018YFD0300701). The supporters did not play any role in the design analysis, or interpretation of this study and the relevant data.

Author's contributions

QF, YXW, ZSM, and HDX conceived and designed the experiments. QF, XFD, HY, ZJM, and SM performed the experiments. QF and YXW analyzed the data. QF, YXW, ZM, and HDX drafted and revised the manuscript. All authors read and approved the manuscript.

Acknowledgements

We are grateful to Professor Honglian Li, Shengli Ding, and Feng Chen from Henan Agricultural University for providing materials and guidance on the experiment. We also thank LetPub for language editing of this manuscript.

Author details

[1] College of Agronomy, Henan Agricultural University/ National Engineering Research Center for Wheat/ Co-construction State Key Laboratory of Wheat and Maize Crop Science, 15 Longzihu College District, Zhengzhou 450046,China.

[2] College of Plant Protection, Henan Agricultural University, Zhengzhou, Henan 450002, China.

References

1. Kazan K, Gardiner DM: **Fusarium crown rot caused by *Fusarium pseudograminearum* in cereal crops: recent progress and future prospects.** *Plant Pathol.* 2018; 19(7):1547-1562. doi.org/10.1111/mpp.12639
2. Knight NL, Sutherland MW: **Histopathological assessment of *Fusarium pseudograminearum* colonization of cereal culms during crown rot infections.** *Plant Dis*. 2016; 100(2):252-259. doi.org/10.1094/PDIS-04-15-0476-RE
3. Liu CJ, Ogbonnaya FC: **Resistance to Fusarium crown rot in wheat and barley: a review.***Plant Breed.* 2015; 134(4):365-372. doi.org/10.1111/pbr.12274
4. Percy CD, Wildermuth GB, Sutherland MW: **Symptom development proceeds at different rates in susceptible and partially resistant cereal seedlings infected with *Fusarium pseudograminearum.***Austral Plant Pathol.* 2012; 41(6):621-631. doi.org/10.1007/s13313-012-0146-2
5. Smiley RW, Gourlie JA, Easley SA, Patterson LM, Whittaker RG: **Crop damage estimates for crown rot of wheat and barley in the Pacific Northwest.***Plant Dis.* 2005; 89(6):595-604. doi.org/10.1094/PD-89-0595
6. Murray GM, Brennan JP: **Estimating disease losses to the Australian barley industry.** *Plant Pathol.* 2010; 39:85-96. doi.org/10.1071/AP09064
7. Klein TA, Burgess LW, Ellison FW, Klein TA, Burgess LW, Ellison FW: **The incidence and spatial patterns of wheat plants infected by *Fusarium graminearum* Group 1 and the effect of crown rot on yield.***Aust J Agric Res.* 1991; 42:399-407. doi.org/10.1071/AR9910399
8. Li HL, Yuan HX, Fu B, Xing XP, Tang WH: **First report of *Fusarium pseudograminearum* causing crown rot of wheat in Henan, China.***Plant Dis.* 2012; 96(7):1065-1065. doi.org/10.1094/PDIS-01-12-0007-PDN
9. Gardiner DM, Benfield AH, Stiller J, Stephen S, Aitken K, Liu C, Kazan K: **A High-resolution genetic map of the cereal crown rot pathogen *Fusarium pseudograminearum* provides a near-complete genome assembly.** *Plant Pathol.* 2018; 19(1):217-226.

doi.org/10.1111/mpp.12519

10. Zhang XT, Gao F, Zhang F, Xie Y, Zhou L, Yuan HX, Zhang S, Li HL: **The complete genomic sequence of a novel megabirnavirus from *Fusarium pseudograminearum*, the causal agent of wheat crown rot.** *Virol*. 2018; 163(11):3173-3175. doi.org/10.1007/s00705-018-3970-z
11. Zhou HF, He XL, Wang S, Ma QZ, Sun B J, Ding SL, Chen L, Zhang M, Li HL: **Diversity of the Fusarium pathogens associated with crown rot in the Huanghuai wheat-growing region of China.** *Microbiol*. 2019; 21(8):2740-2754. doi.org/10.1111/1462-2920.14602
12. Chen LL, Geng XJ, Ma YM, Zhao JY, Chen WB, Xing XP, Shi Y, Sun BJ, Li HL: **The ER lumenal Hsp70 protein FpLhs1 is important for conidiation and plant infection in *Fusarium pseudograminearum*.***Front Microbiol*. 2019; 10:1401. doi.org/10.3389/fmicb.2019.01401
13. Chen LL, Ma YM, Zhao JY, Geng XJ, Chen WB, Ding SL, Li HL: **The bZIP transcription factor FpAda1 is essential for fungal growth and conidiation in *Fusarium pseudograminearum*.***Curr Genet*. 2020; 66(3):507-515. doi.org/10.1007/s00294-019-01042-1
14. Kang RJ, Li GN, Zhang MJ, Zhang PP, Wang LM, Zhang YS, Chen LL, Yuan HX, Ding SL, Li HL: **Expression of *Fusarium pseudograminearum* FpNPS9 in wheat plant and its function in pathogenicity.** *Genet*. 2020; 66(1):229-243. doi.org/10.1007/s00294-019-01017-2
15. Pariyar SR, Erginbas-Orakci G, Dadshani S, Chijioke OB, Léon J, Dababat AA, Grundler FMW: **Dissecting the genetic complexity of Fusarium crown rot resistance in wheat.** *Sci Rep* 2020; 10(1):3200. doi.org/10.1038/s41598-020-60190-4
16. Poole GJ, Smiley RW, Paulitz TC, Walker CA, Carter AH, See DR, Garland-Campbell K: **Identification of quantitative trait loci (QTL) for resistance to Fusarium crown rot (*Fusarium pseudograminearum*) in multiple assay environments in the Pacific Northwestern US.***Theor Appl Genet*. 2012; 125(1):91-107. doi.org/10.1007/s00122-012-1818-6
17. Ceoloni C, Forte P, Kuzmanović L, Tundo S, Moscetti I, De Vita P, Virili ME, D'Ovidio R: **Cytogenetic mapping of a major locus for resistance to Fusarium head blight and crown rot of wheat on *Thinopyrum elongatum* 7EL and its pyramiding with valuable genes from a *ponticum* homoeologous arm onto bread wheat 7DL.***Theor Appl Genet*. 2017; 130(10):2005-2024. doi.org/10.1007/s00122-017-2939-8
18. Yang X, Pan Y, Singh PK, He X, Ren Y, Zhao L, Zhang N, Cheng S, Chen F: **Investigation and genome-wide association study for Fusarium crown rot resistance in Chinese common wheat.***BMC Plant Biol*. 2019; 19: doi.org/10.1186/s12870-019-1758-2
19. Blum A, Benfield AH, Sørensen JL, Nielsen MR, Bachleitner S, Studt L, Beccari G, Covarelli L, Batley J, Gardiner DM: **Regulation of a novel Fusarium cytokinin in *Fusarium pseudograminearum*.***Fungal Biol.* 2019; 123(3):255-266. org/10.1016/j.funbio.2018.12.009
20. Sørensen JL, Benfield AH, Wollenberg RD, Westphal K, Wimmer R, Nielsen MR, Nielsen KF, Carere J, Covarelli L,Beccari G, Powell J, Yamashino T, Kogler H, Sondergaard TE, Gardiner DM: **The cereal pathogen *Fusarium pseudograminearum* produces a new class of active cytokinins during infection.** *Plant Pathol*. 2018; 19(5):1140-1154. doi.org/10.1111/mpp.12593
21. Carlson R, Tugizimana F, Steenkamp PA, Dubery IA, Labuschagne N: **Differential metabolic reprogramming in *Paenibacillus alvei*-primed *Sorghum bicolor* seedlings in response to *Fusarium pseudograminearum*** *Metabolites*. 2019; 9(7):150. doi.org/10.3390/metabo9070150
22. Desmond OJ, Edgar CI, Manners JM, Maclean DJ, Schenk PM, Kazan K: **Methyl jasmonate induced gene expression in wheat delays symptom development by the crown rot pathogen *Fusarium pseudograminearum*.** *Mol. Plant Pathol.* 2005; 67(3-5):171-179. doi.org/10.1016/j.pmpp.2005.12.007
23. Desmond OJ, Manners JM, Schenk PM, Maclean DJ, Kazan K: **Gene expression analysis of the wheat response to infection by *Fusarium pseudograminearum*.** *Mol. Plant Pathol.* 2008; 73(1-3):40-47. doi.org/10.1016/j.pmpp.2008.12.001
24. Powell JJ, Carere J, Fitzgerald TL, Stiller J, Covarelli L, Xu Q, Gubler F, Colgrave ML, Gardiner DM, Manners JM, Henry RJ, Kazan K: **The Fusarium crown rot pathogen *Fusarium pseudograminearum* triggers a suite of transcriptional and metabolic changes in bread wheat (*Triticum aestivum*).***Ann. Bot*. 2017; 119(5):853-867. doi.org/10.1093/aob/mcw207
25. Weltmeier F, Ehlert A, Mayer CS, Dietrich K, Wang X, Schutze K, Alonso R, Harter K, Vicente-Carbajosa J, Droge-Laser W: **Combinatorial control of Arabidopsis proline dehydrogenase transcription by specific heterodimerisation of bZIP transcription factors.***EMBO J* 2006; 25(13):3133-3143. org/10.1038/sj.emboj.7601206
26. Shen Y, Du J, Yue L, Zhan X: **Proteomic analysis of plasma membrane proteins in wheat roots exposed to phenanthrene.** *Sci. Pollut. Res.* 2016; 23(11):10863-10871. doi.org/10.1007/s11356-016-6307-z
27. Wang Y, Xu L, Tang MJ, Jiang HY, Chen W, Zhang W, Wang RH, Liu LW: **Functional and integrative analysis of the proteomic profile of radish root under Pb exposure.** *Plant. Sci.* 2016; 7:1871. doi.org/10.3389/fpls.2016.01871

28. Piero ARL, Mercurio V, Puglisi I, Petrone G: **Gene isolation and expression analysis of two distinct sweet orange [*Citrus sinensis* (Osbeck)] tau-type glutathione transferases.***Gene* 2009; 443(1-2):143-150. doi.org/10.1016/j.gene.2009.04.025
29. Yasir M, He SP, Sun GF, Geng XL, Pan Z, Gong WF, Jia YH, Du XM: **A Genome-Wide association study revealed key SNPs/Genes associated with salinity stress tolerance in upland cotton.***Genes* 2019; 10(10):829. doi.org/10.3390/genes10100829
30. Islam MDS, Choudhury M, Majlish AK, Islam T, Ghosh A: **Comprehensive genome-wide analysis of Glutathione S-transferase gene family in potato (*Solanum tuberosum*) and their expression profiling in various anatomical tissues and perturbation conditions.***Gene* 2018; 639:149-162. doi.org/10.1016/j.gene.2017.10.007
31. Hause B, Maier W, Miersch O, Kramell R, Strack D: **Induction of jasmonate biosynthesis in arbuscular mycorrhizal barley roots.***Plant Physiol.* 2002; 130(3):1213-1220. doi.org/10.1104/pp.006007
32. Schaller F, Schaller A, Stintz A: **Biosynthesis and metabolism of jasmonates.** *Plant Growth Regul.* 2005; 23(3):179-199. doi.org/10.1007/s00344-004-0047-x
33. De Domenico S, Bonsegna S, Horres R, Pastor V, Taurino M, Poltronieri P, Imtiaz M, Kahl G, Flors V, Winter P, Santino A: **Transcriptomic analysis of oxylipin biosynthesis genes and chemical profiling reveal an early induction of jasmonates in chickpea roots under drought stress.***Plant Physiol. Biochem.* 2012; 61:115-122. doi.org/10.1016/j.plaphy.2012.09.009
34. Naqvi RZ, Zaidi SS, Mukhtar MS, Amin I,Mishra B, Strickler S, Mueller LA, Asif M, Mansoor S: **Transcriptomic analysis of cultivated cotton *Gossypium hirsutum* provides insights into host responses upon whitefly-mediated transmission of cotton leaf curl disease.***PLoS One* 2019; 14(2): e0210011. doi.org/10.1371/journal.pone.0210011
35. Alazem M, Lin NS: **Roles of plant hormones in the regulation of host-virus interactions.***Plant Pathol.* 2015; 16(5):529-540. doi.org/10.1111/mpp.12204
36. Kojima S, Konishi N, Beier MP, Ishiyama K, Maru I, Hayakawa T, Yamaya T: **NADH-dependent glutamate synthase participated in ammonium assimilation in Arabidopsis root.***Plant Signal Behav.* 2014; 9(8):e29402. doi.org/10.4161/psb.29402
37. Mauriat M, Leplé JC, Claverol S, Bartholomé J, Negroni L, Richet N, Lalanne C, Bonneu M, Coutand C, Plomion C: **Quantitative proteomic and phosphoproteomic approaches for deciphering the signaling pathway for tension wood formation in poplar.** *Proteome Res.* 2015; 14(8):3188-3203. doi.org/10.1021/acs.jproteome.5b00140
38. Ma QP, Li H, Zou ZW, Arkorful E, Lv QR, Zhou QQ, Chen X, Sun K, Li XH: **Transcriptomic analyses identify albino-associated genes of a novel albino tea germplasm 'Huabai 1'.***Hortic Res.-England* 2018; 5:54. doi.org/10.1038/s41438-018-0053-y
39. Reinprecht Y, Yadegari Z, Perry GE, Siddiqua M, Wright LC, McClean PE, Pauls KP: **In silico comparison of genomic regions containing genes coding for enzymes and transcription factors for the phenylpropanoid pathway in *Phaseolus vulgaris* and *Glycine max* L. Merr.***Front. Plant. Sci.* 2013; 4:317. doi.org/10.3389/fpls.2013.00317
40. Morris JS, Caldo KMP, Liang S, Facchini PJ: **PR10/Bet v1-like proteins as novel contributors to plant biochemical diversity.** *Chembiochem*. 2020. doi.org/ 10.1002/cbic.202000354
41. Cao Y, Han Y, Meng D, Li D, Jin Q, Lin Y, Cai Y: **Structural, evolutionary, and functional analysis of the class iii peroxidase gene family in Chinese pear (*Pyrus bretschneideri*)**. *Plant. Sci.* 2016; 7:1874. doi.org/10.3389/fpls.2016.01874
42. Proietti S, Bertini L, Van der Ent S, Leon-Reyes A, Pieterse CM, Tucci M, Caporale C, Caruso C: **Cross activity of orthologous WRKY transcription factors in wheat and Arabidopsis.** *Exp. Bot.* 2011; 62(6):1975-1990. doi.org/10.1093/jxb/erq396
43. Hollbacher B, Schmitt AO, Hofer H, Ferreira F, Lackner P: **Identification of proteases and protease inhibitors in allergenic and non-allergenic pollen.** *J. Mol. Sci.* 2017; 18(6):1199. doi.org/10.3390/ijms18061199
44. Breen S, Williams SJ, Outram M, Kobe B, Solomon PS: **Emerging insights into the functions of pathogenesis-related protein 1.***Trends Plant Sci.* 2017; 22(10):871-879. doi.org/10.1016/j.tplants.2017.06.013
45. Gamir J, Darwiche R, Van't Hof P, Choudhary V, Stumpe M, Schneiter R, Mauch F: **The sterol-binding activity of pathogenesis-related protein 1 reveals the mode of action of an antimicrobial protein.***Plant J.* 2017; 89(3):502-509. doi.org/10.1111/tpj.13398
46. Wu SW, Wang HW, Yang ZD, Kong LR: **Expression comparisons of pathogenesis-related (PR) genes in wheat in response to infectioninfestation by Fusarium,Yellow dwarf virus (YDV) aphid-transmitted and Hessian Fly.** *Integr. Agric.* 2014; 13:926-936. doi.org/10.1016/S2095-3119(13)60570-5
47. Zhang JR, Wang F, Liang F, Zhang YJ, Ma LS, Wang HY, Liu DQ: **Functional analysis of a pathogenesis-related thaumatin-like protein gene TaLr35PR5 from wheat induced by leaf rust fungus.***BMC Plant Biol.* 2018; 18(1):76. doi.org/10.1186/s12870-018-1297-2
48. Lu SW, Faris JD, Sherwood R, Friesen TL, Edwards MC: **A dimeric PR-1-type pathogenesis-related protein interacts with ToxA and potentially mediates ToxA-induced necrosis in sensitive wheat.** *Plant Pathol.* 2014; 15(7):650-663. doi.org/10.1111/mpp.12122

49. Wang XB, Chen XZ, Li JR, Zhou XX, Liu YT, Zhong LT, Tang Y, Zheng H, Liu JY, Zhan RT, Chen LK: **Global analysis of lysine succinylation in patchouli plant leaves.***Hortic Res.-England* 2019; 6:133. doi.org/10.1038/s41438-019-0216-5
50. Swarbrick PJ, Schulze-Lefert P, Scholes JD: **Metabolic consequences of susceptibility and resistance (race-specific and broad-spectrum) in barley leaves challenged with powdery mildew.***Plant Cell Environ.* 2006; 29(6):1061-1076. doi.org/10.1111/j.1365-3040.2005.01472.x
51. Restrepo S, Myers KL, Del PO, Martin GB, Hart AL, Buell CR, Fry WE, Smart CD: **Gene profiling of a compatible interaction between *Phytophthora infestans* and *Solanum tuberosum* suggests a role for carbonic anhydrase.** *Plant-Microbe Interact.* 2005; 18:913-922. doi.org/10.1094/MPMI-18-0913
52. Moy P, Qutob D, Chapman BP, Atkinson I, Gijzen M: **Patterns of gene expression upon infection of soybean plants by *Phytophthora sojae*.** *Plant-Microbe Interact.* 2004; 17:1051-1062. doi.org/10.1094/MPMI.2004.17.10.1051
53. Missihoun TD, Kotchoni SO, Bartels D: **Aldehyde dehydrogenases function in the homeostasis of pyridine nucleotides in *Arabidopsis thaliana*.***Sci Rep* 2018; 8(1):2936. doi.org/10.1038/s41598-018-21202-6
54. Du DF, Gao X, Geng J, Li QY, Li L, Lv Q, Li XJ: **Identification of key proteins and networks related to grain development in wheat (*Triticum aestivum*) by comparative transcription and proteomic analysis of allelic variants in *TaGW2-6A*.***Front. Plant. Sci*. 2016; 7:922. doi.org/10.3389/fpls.2016.00922
55. Lefebvre S, Lawson T, Zakhleniuk OV, Lloyd JC, Raines CA, Fryer M: **Increased sedoheptulose-1,7-bisphosphatase activity in transgenic tobacco plants stimulates photosynthesis and growth from an early stage in development.***Plant Physiol.* 2005; 138(1):451-460. doi.org/10.1104/pp.104.055046
56. Meng FJ, Luo QX, Wang QY, Zhang XL, Qi ZH, Xu FL, Lei X, Cao Y, Chow WS, Sun GY: **Physiological and proteomic responses to salt stress in chloroplasts of diploid and tetraploid black locust (*Robinia pseudoacacia*).***Sci Rep* 2016; 6:23098. doi.org/10.1038/srep23098
57. Long RC, Li MN, Zhang TJ, Kang JM, Sun Y, Cong LL, Gao YL, Liu FQ, Yang QC: **Comparative proteomic analysis reveals differential root proteins in *Medicago sativa* and *Medicago truncatula* in response to salt stress.** *Plant. Sci*. 2016; 7:424. doi.org/10.3389/fpls.2016.00424
58. Caruso G, Cavaliere C, Foglia P, Gubbiotti R, Samperi R, Lagana A: **Analysis of drought responsive proteins in wheat (*Triticum durum*) by 2D-PAGE and MALDI-TOF mass spectrometry.***Plant Sci.* 2009; 177(6):570–576. doi.org/10.1016/j.plantsci.2009.08.007
59. Merewitz EB, Gianfagna T, Huang B: **Protein accumulation in leaves and roots associated with improved drought tolerance in creeping bentgrass expressing an *ipt* gene for cytokinin synthesis.** *Exp. Bot*. 2011; 62(15):5311-5333. doi.org/10.1093/jxb/err166
60. Li J, Yang XW, Liu XH, Yu HB, Du CY, Li MD, He DX: **Proteomic analysis of the compatible interaction of wheat and powdery mildew (*Blumeria graminis f. sp. tritici*).***Plant Physiol. Biochem.* 2017; 111:234-243. doi.org/10.1016/j.plaphy.2016.12.006
61. Wang X, Zhang W, Hao Z, Li X, Zhang Y, Wang S: *Principles and Techniques of Plant Physiological Biochemical Experiment*. Beijing, China:Higher Education Press; 2015.
62. Cao XC, Wu LL, Wu MY, Zhu CQ, Jin QY, Zhang JH: **Abscisic acid mediated proline biosynthesis and antioxidant ability in roots of two different rice genotypes under hypoxic stress.***BMC Plant Biol*. 2020; 20(1):198. doi.org/10.1186/s12870-020-02414-3
63. Li H, Sun Q, Zhao S, Zhang W: *Principles and Techniques of Plant Physiological Biochemical Experiment*. Beijing, China:Higher Education Press; 2000.
64. Yu JJ, Chen SX, Zhao Q, Wang T, Yang CP, Diaz C, Sun GR, Dai SJ: **Physiological and proteomic analysis of salinity tolerance in *Puccinellia tenuiflora*.***J Proteome Res*. 2011; 10(9):3852-3870. doi.org/10.1021/pr101102p
65. Zhang LT, Xin ZY, Yu X, Ma C, Liang WW, Zhu MC, Cheng QW, Li ZZ, Niu YN, Ren YZ, Wang ZQ, Lin TB: **Osmotic stress induced cell death in wheat is alleviated by tauroursodeoxycholic acid and involves endoplasmic reticulum stress-related gene expression.** *Plant. Sci*. 2017; 8:667. doi.org/10.3389/fpls.2017.00667
66. Su XY, Fan XC, Shao RX, Guo J, Wang YC, Yang JP, Yang QH, Guo L: **Physiological and iTRAQ-based proteomic analyses reveal that melatonin alleviates oxidative damage in maize leaves exposed to drought stress.***Plant Physiol. Biochem*. 2019; 142:263–274. doi.org/10.1016/j.plaphy.2019.07.012
67. Bradford MM: **A rapid and sensitive method for the quantification of microgram quantities of protein utilizing the principles of protein dye binding.** *Biochem*. 1976; 72(s1-2):248-254. doi.org/10.1016/0003-2697(76)90527-3
68. Livak KJ, Schmittgen TD: **Analysis of relative gene expression data using real-time quantitative PCR and the $2^{-\Delta\Delta CT}$***Methods* 2001; 25(4):402-408. doi.org/10.1006/meth.2001.1262

Tables

Table 1. The mRNA and protein abundance changes of 16 selected genes in the study.

Gene names	S1_3dpi vs S1_0dpi				S2_3dpi vs S2_0dpi			
	Gene fold changes	Regulated type	Protein fold changes	Regulated type	Gene fold changes	Regulated type	Protein fold changes	Regulated type
GLU1B	0.25	Down	0.46	Down	0.15	Down	0.48	Down
NMT1	2.70	Up	1.68	Up	0.74	Down	1.78	Up
XIPI	1.46	Up	0.58	Down	0.34	Down	0.64	Down
cla30	2.41	Up	2.25	Up	-	-	-	-
gstu2	15.48	Up	2.27	Up	-	-	-	-
Pr-1-2	4.18	Up	7.00	Up	-	-	-	-
Pr-1-1	8.43	Up	6.08	Up	-	-	-	-
PR-1.2	29.84	Up	2.35	Up	-	-	-	-
LIM	-	-	-	-	2.21	Up	1.69	Up
psaC	-	-	-	-	1.15	Up	2.13	Up
petD	-	-	-	-	1.19	Up	1.66	Up
rps11	-	-	-	-	1.94	Up	1.56	Up
CENH3	-	-	-	-	2.44	Up	1.73	Up
ltp9.4b	-	-	-	-	1.81	Up	1.51	Up
TRAES_3BF087500010CFD_c1	-	-	-	-	1.10	Up	2.51	Up
TRAES_3BF088300010CFD_c1	-	-	-	-	1.21	Up	2.51	Up

Figures

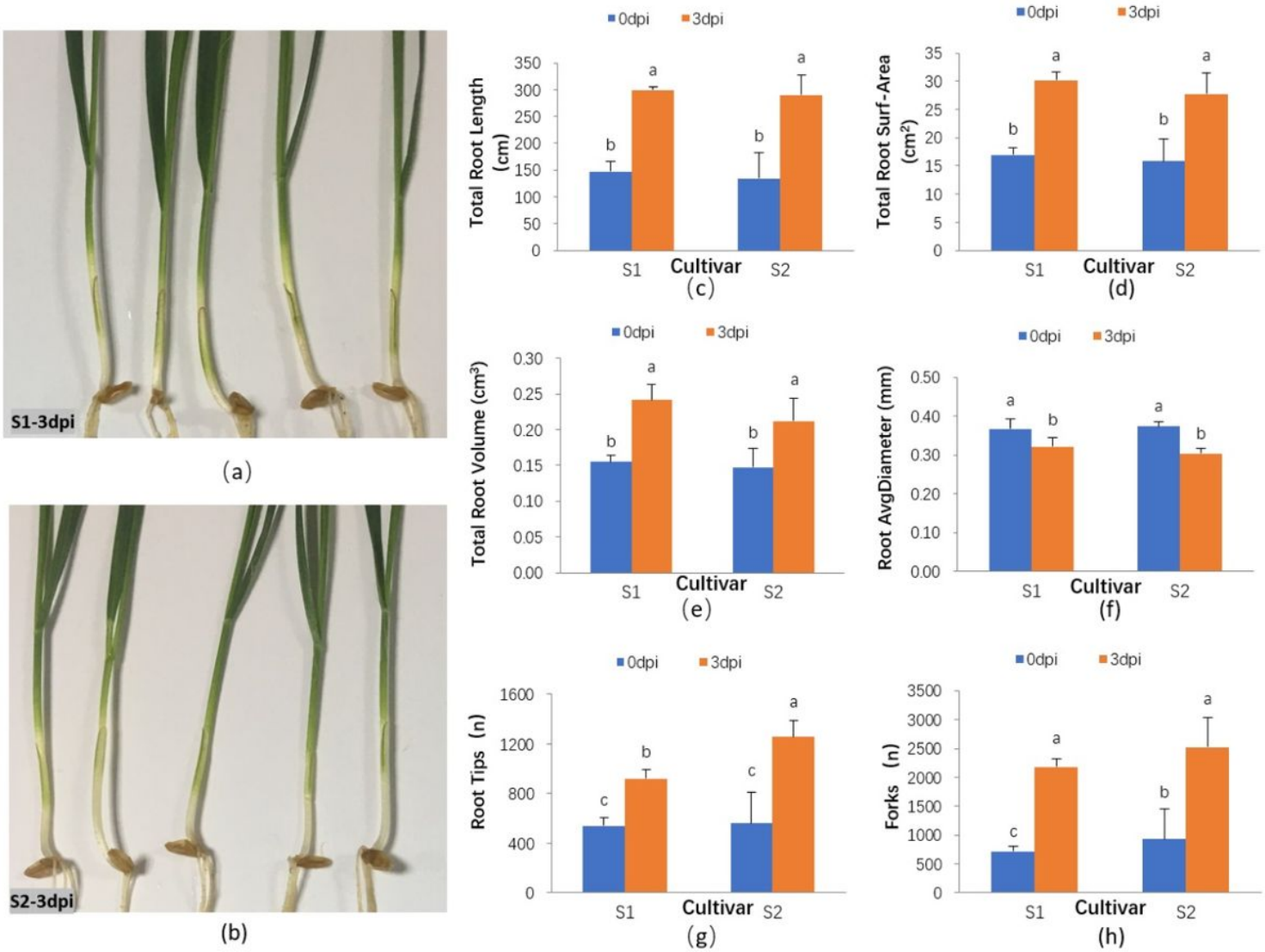

Figure 1

Phenotypical and morphological parameters in response to Fusarium pseudograminearum infection in wheat. Data are shown as mean ± SD (n = 10) of three independent experiments. Different small letters (a or b) indicate significant difference between the groups ($P < 0.05$). S1 represent UC1110, S2 represent PI610750.

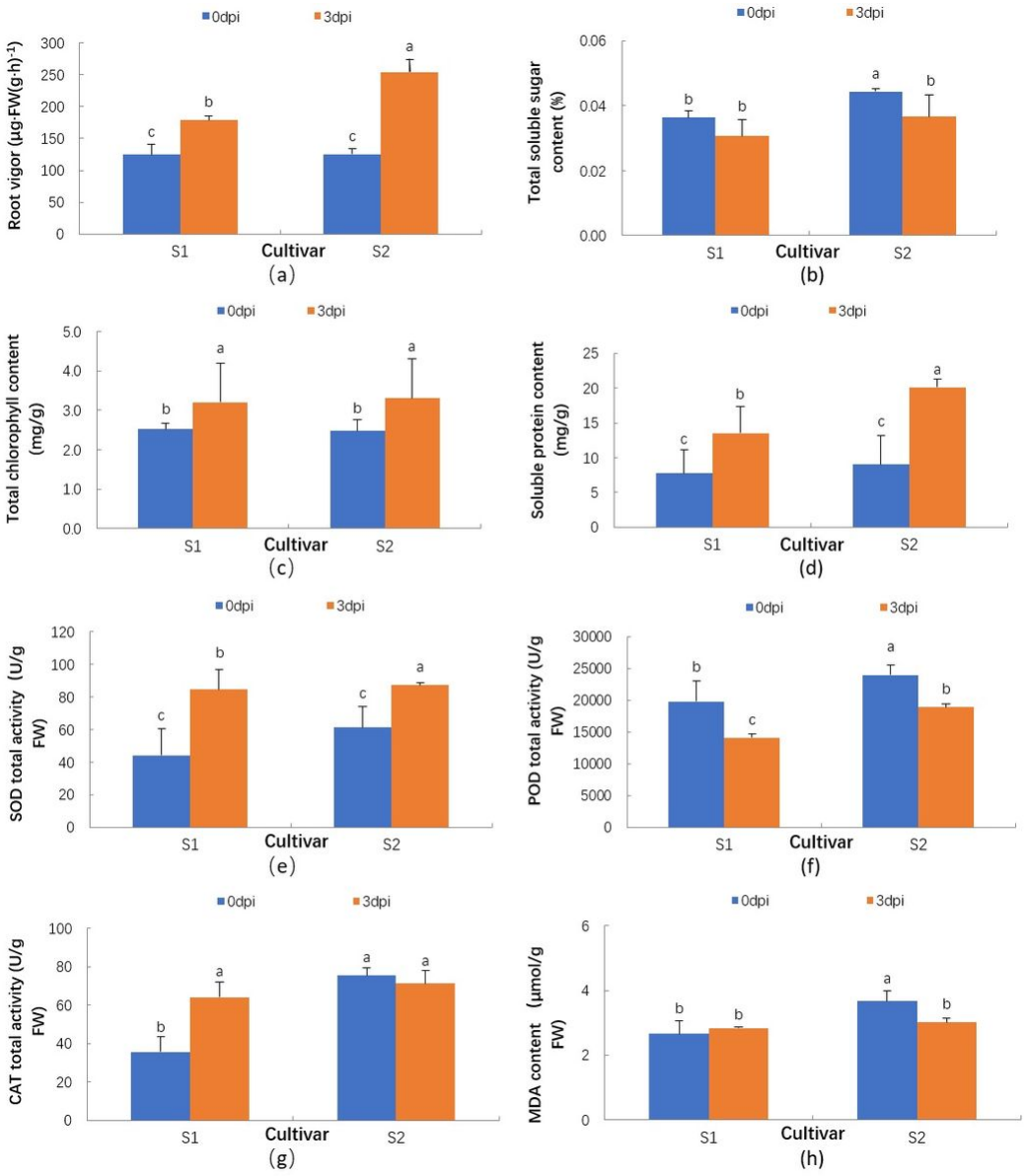

Figure 2

Physiological and biochemical parameters in response to F. pseudograminearum infection in wheat. Data are shown as mean ± SD (n = 4) of three independent experiments. Different lowercase letters (a or b) indicate significant differences between the groups ($P < 0.05$). S1 represents UC1110, S2 represents PI610750.

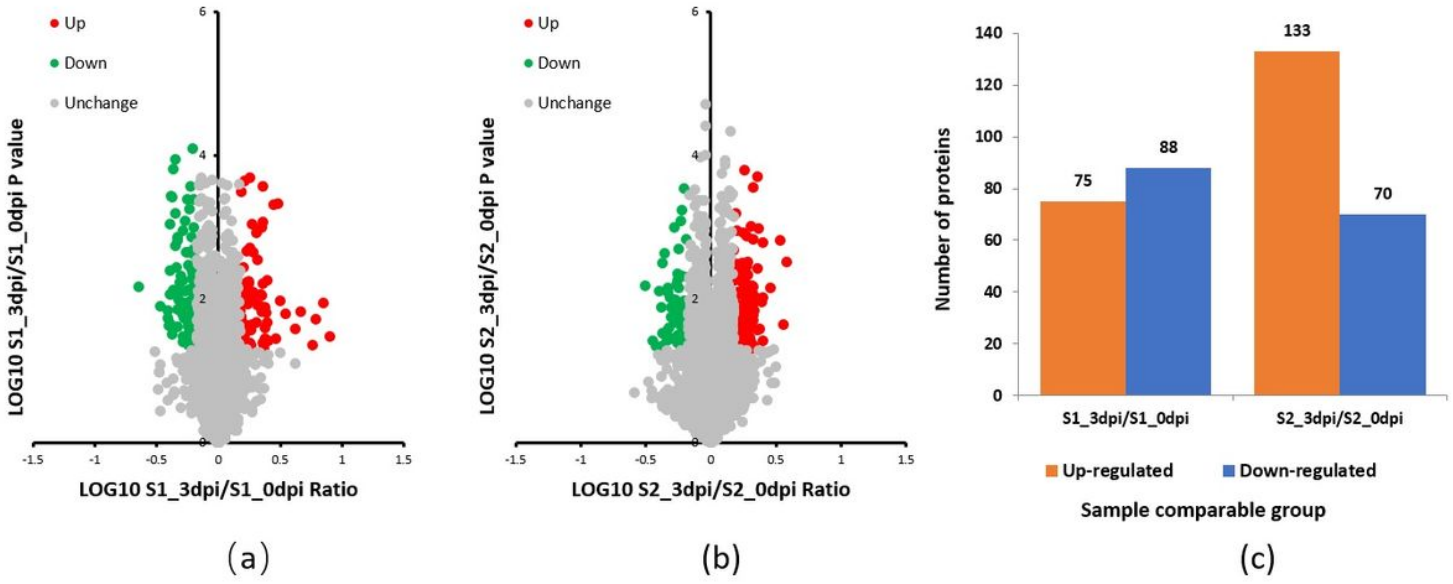

Figure 3

Differentially expressed proteins (DEPs) analysis between S1-3dpi/S1-0dpi and S2-3dpi/S2-0dpi. Volcano plot of all DEPs in S1-3dpi/S1-0dpi (a) and S2-3dpi/S2-0dpi (b); Quantitative analysis of the proteome between S1-3dpi/S1-0dpi and S2-3dpi/S2-0dpi (c). In blue (down-regulated): DEPs with $p < 0.05$ and fold change < 0.667; in orange (up-regulated): DEPs with $p < 0.05$ and fold change > 1.5. S1 represents UC1110, S2 represents PI610750.

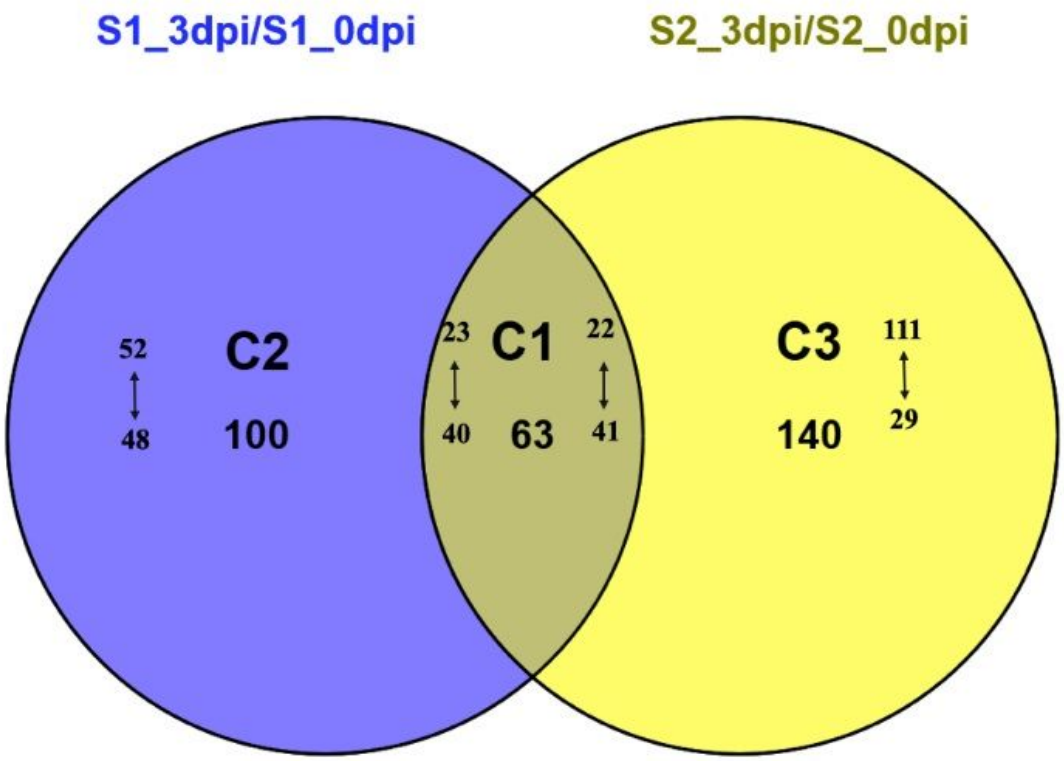

Figure 4

Venn diagram of the distribution of DEPs in S1-3dpi/S1-0dpi and S2-3dpi/S2-0dpi. The circles are proportional to the number of proteins identified in each treatment. The overlapping regions indicate the number of common proteins. The ↑ indicates up-regulated, ↓ indicates down-regulated. S1 represents UC1110, S2 represents PI610750.

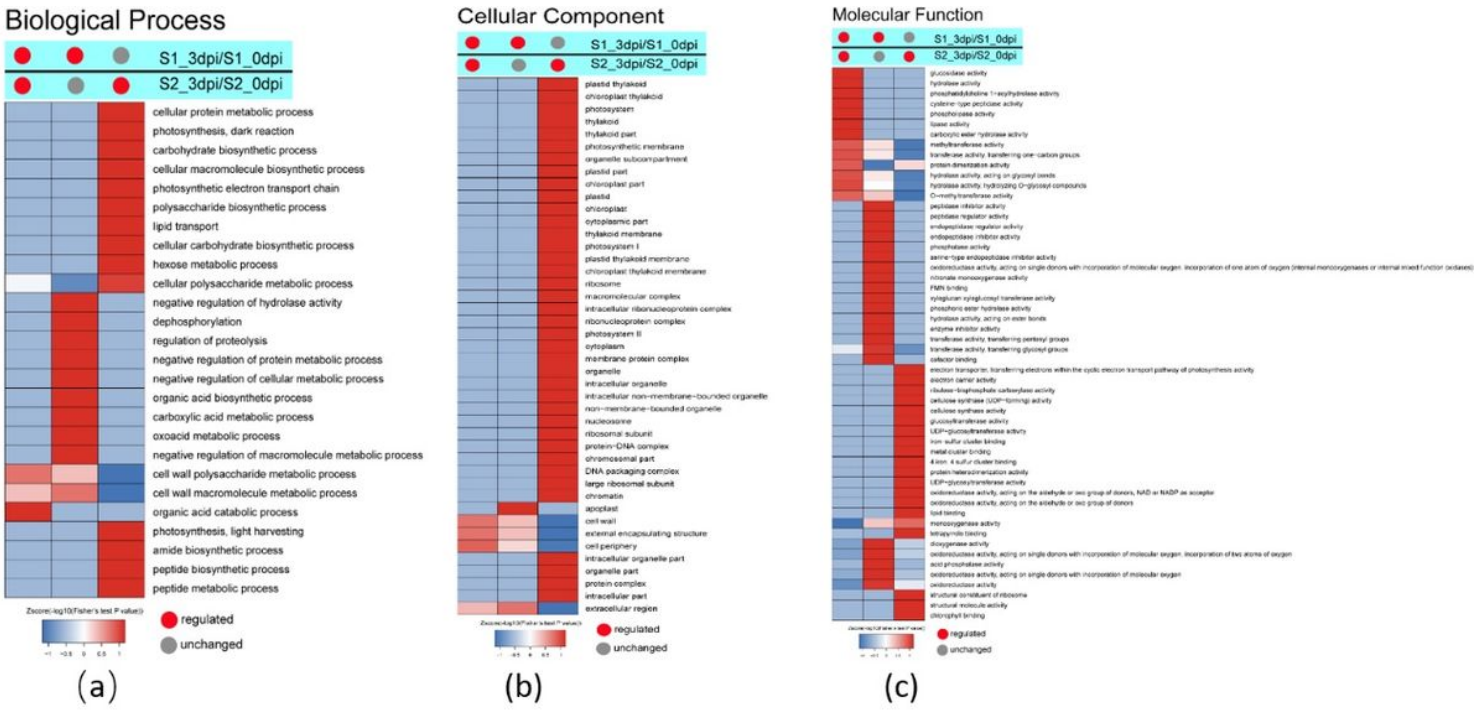

Figure 5

GO-functional enrichment cluster analysis of DEPs: (a) biological process enrichment analysis; (b) cellular component enrichment analysis; (c) molecular functional enrichment analysis. S1 represents UC1110, S2 represents PI610750.

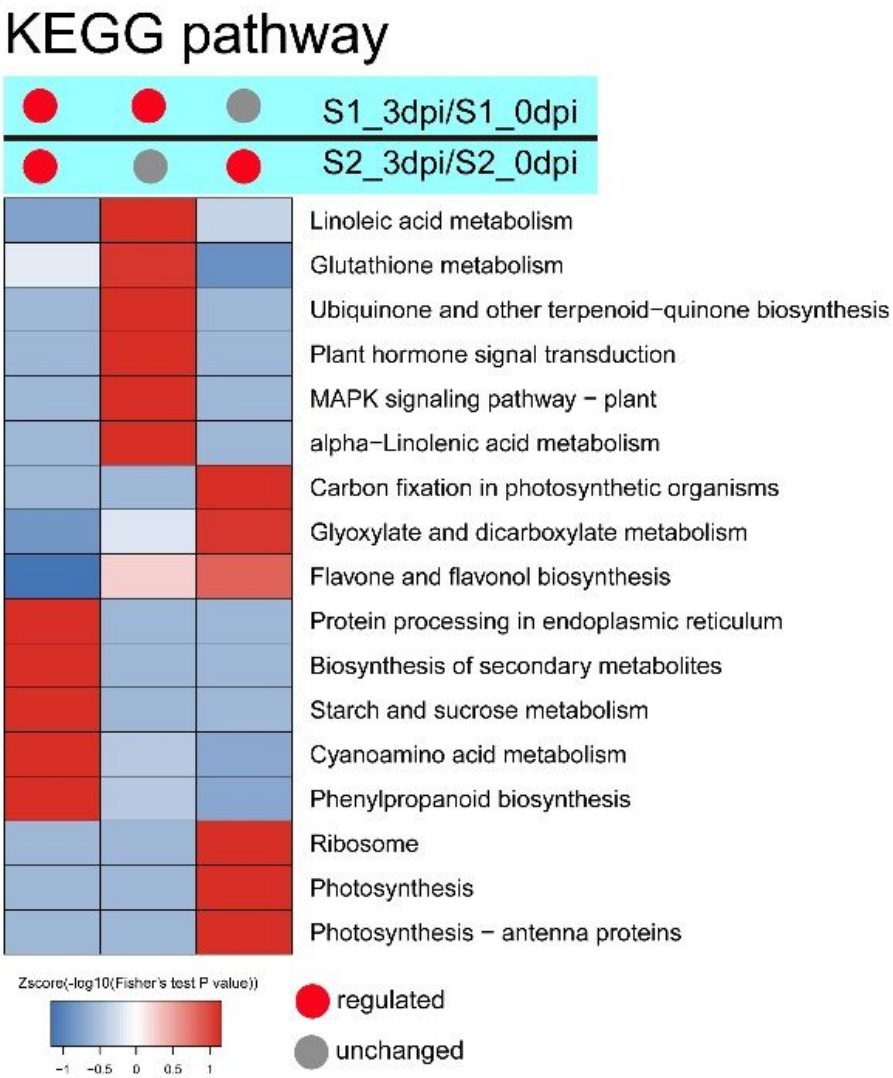

Figure 6

KEGG pathway enrichment cluster analysis of the DEPs of two comparison groups. S1 represents UC1110, S2 represents PI610750.

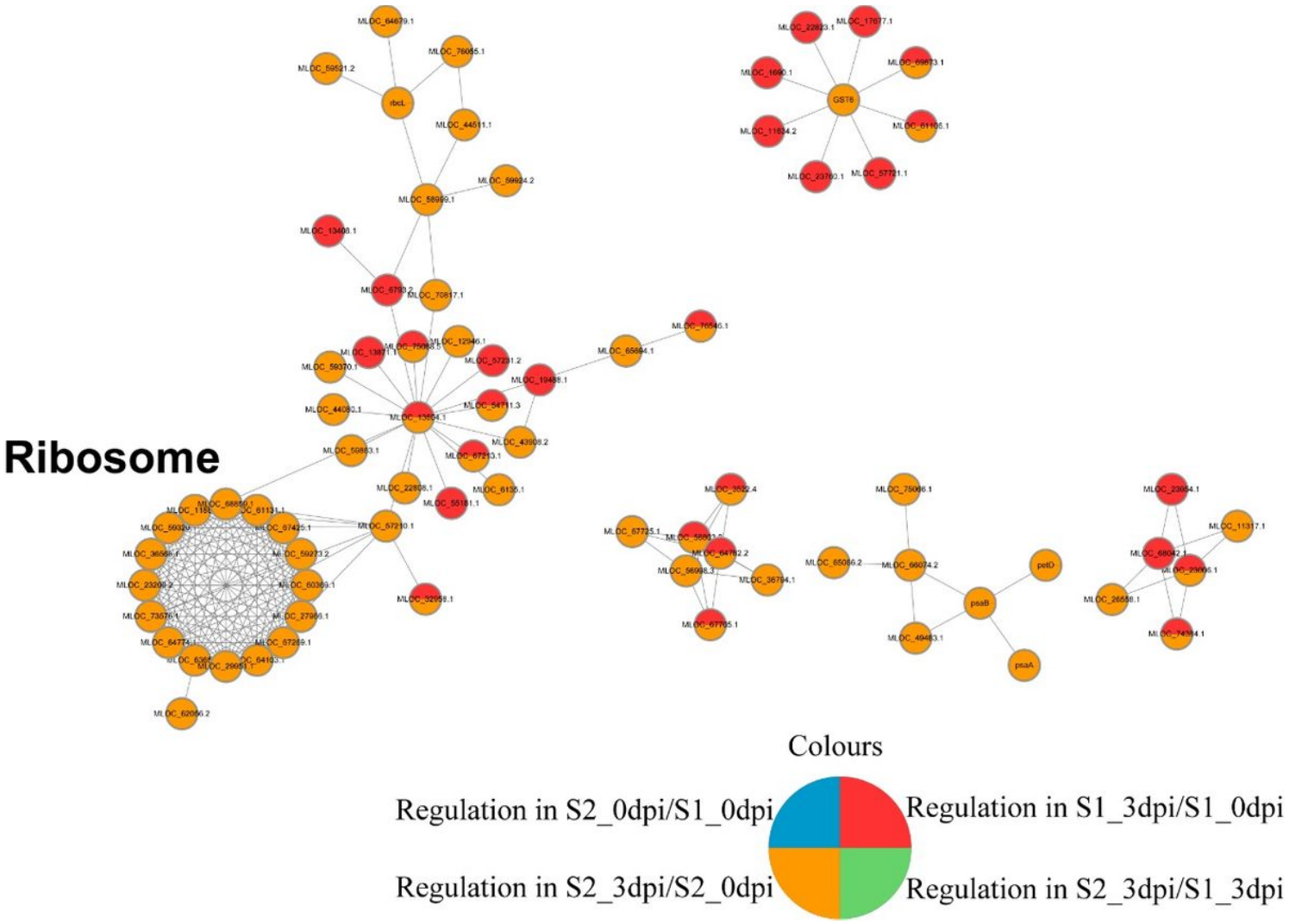

Figure 7

Protein-protein interaction network analysis of the DEPs of two comparison groups.

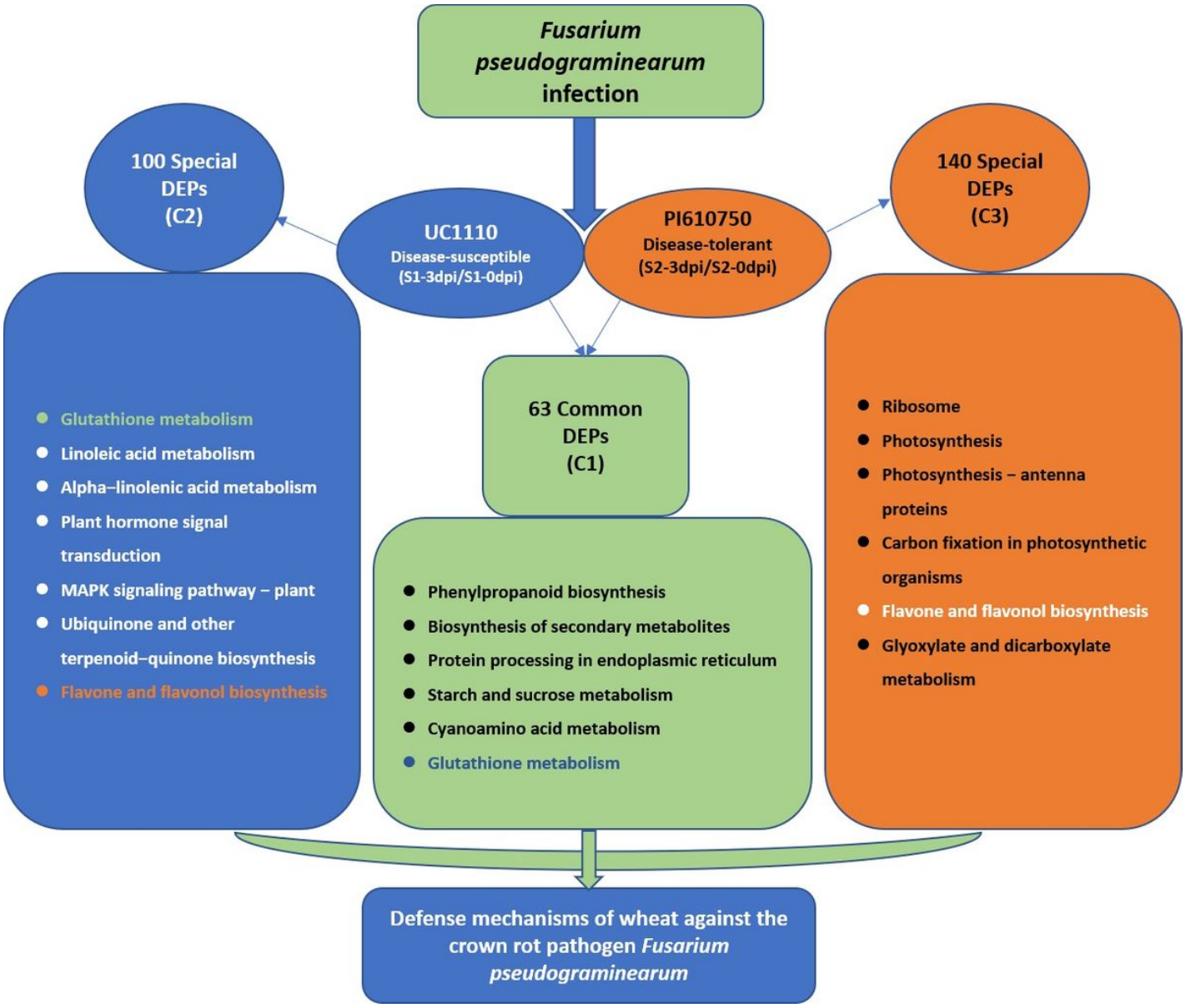

Figure 8

Schematic model of the defense mechanisms of wheat against the crown rot pathogen F. pseudograminearum.

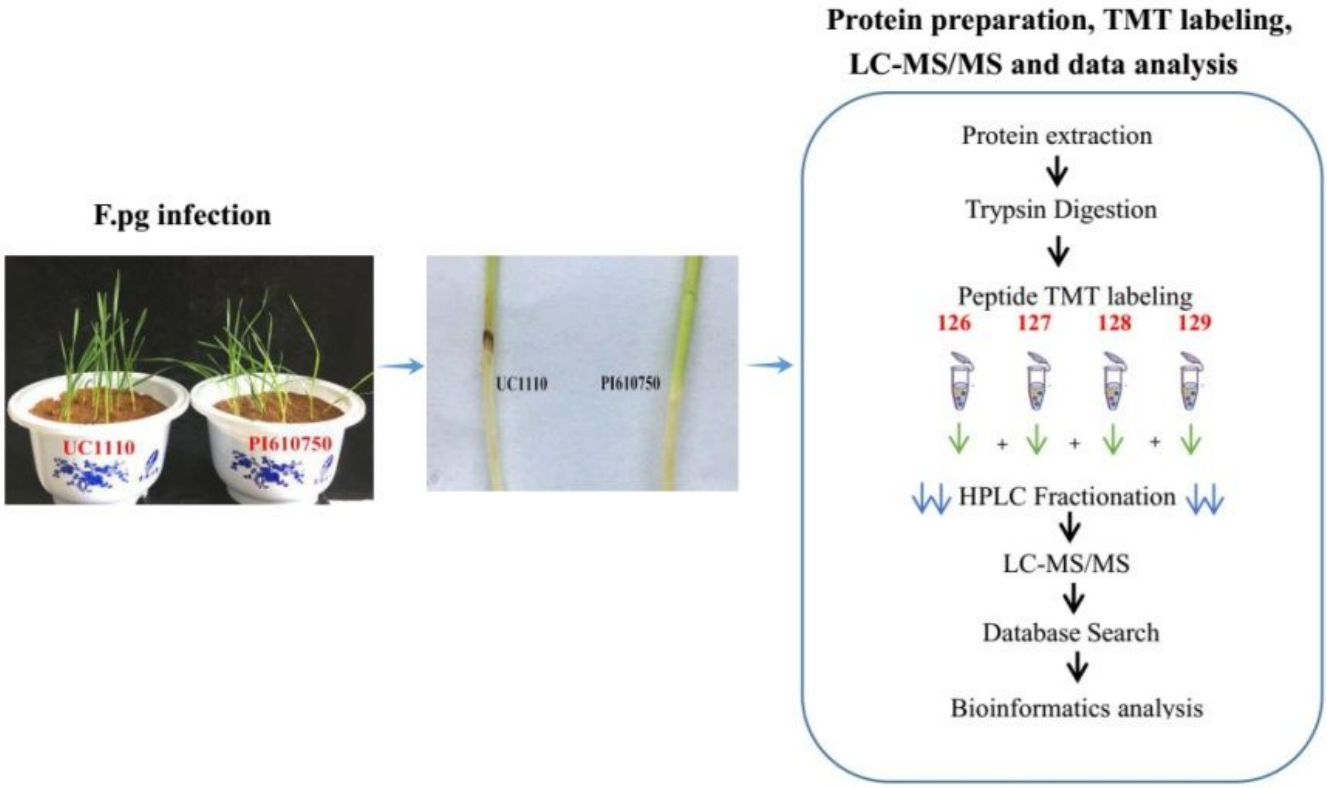

Figure 9

Workflow for the characterization of defense mechanisms of wheat in response to F. pseudograminearum infection using TMT-based quantitative proteomics technology. The stem bases of UC1110 and PI610750 seedlings were inoculated with the colonized grains.

Supplementary Files

This is a list of supplementary files associated with this preprint. Click to download.

- Additionalfiles1.xlsx
- Additionalfiles2.xlsx
- FigureS1.pdf